Semiannual Progress Report

SIMULATIONS OF TURBULENT MIXING AND REACTING FLOWS AND THEIR APPLICATIONS TO TURBULENCE MODELING

Grant NAG-1-532

Department of Mechanical Engineering
Stanford University

Prof. Joel H. Ferziger
Prof. Brian J. Cantwell
Principal Investigators

July 1986

I. Overall Objectives

The principal objective of this project is to apply the method of full simulation to reacting turbulent flows. Full simulation has proven of great value as a complement to experiments for the study of nonreacting turbulent flows. It provides insight into the physics of turbulent flows and their modeling. It is natural to try to extend these methods to the simulation of reacting turbulent flows. Because this is one of the first attempts at this type of simulation, a subsidiary goal of this work is to demonstrate the feasibility of using simulation to study turbulent reacting flows. In addition, we intend to show that such simulations can be used to provide physical insight into the nature of turbulent combustion and to provide data that will help to construct models that can be used in engineering simulations of turbulent reacting flows.

Reacting flows are considerably more difficult to simulate than nonreacting flows. The presence of chemical reaction demands that conservation equations for the various chemical species be solved along with the equations describing the fluid mechanics. Thus, the simulation of combusting flows includes all of the difficulties found in nonreacting turbulent flows as well as an equally large set associated with computing chemically reacting flows. However, experimental measurements are also very difficult to make in reacting turbulent flows, so the benefits produced by a successful simulation are greater; this is a primary motivation for pursuing simulations of this type.

We first had to choose the problems to be considered; this choice is important in any research effort, but even more important in this one, due to

the need for this work to demonstrate the feasibility of the method and to provide the basis for further simulations of a more applied nature. Since the grant supports two student research assistants, two problems had to be selected. The choice was based on the following criteria: (1) relative simplicity of both geometry and chemistry; (2) this is essential in order to provide feasibility of simulation in a reasonable time on current computers; (3) furthermore, to allow careful checking of the results, we need to consider flows for which sufficient experimental data are available; (4) finally, we want problems which, to the extent possible, have relevance to applications. In addition, the problems should be as different from each other as possible. After considerable searching, we selected the reacting axisymmetric jet and turbulent flame propagation. We shall describe the work on each of these problems separately below.

II. Reacting Axisymmetric Jet

A. Physical Description

Shear is fundamental to the mixing of fuel and oxidant in nearly all combustors in which the reactants are not premixed. The presence of strong shear ensures the creation of turbulence that enhances the mixing process; mixing must take place before chemical reaction is possible. In most combustors, the flow configuration is essentially that of an axisymmetric jet; the external air stream may be stationary or moving at a slower speed than the fuel or fuel-air jet. For this reason, we have chosen to study the axisymmetric jet-diffusion flame as one of the initial cases. This flow has been the subject of recent experiments at Stanford, and our knowledge of this flow will be very valuable in helping to simulate it.

The nonreacting axisymmetric jet has not yet been treated by full simulation. However, a related flow, the spatially developing mixing layer, has recently been simulated by one of the members of our group. This flow shares many of the features of the axisymmetric jet but differs in important ways from the time-developing mixing layers that have been simulated by a number of other authors. Several important problems had to be resolved in order to make this simulation. Firstly, the conditions at the upstream boundary of the computational domain have to be specified in full detail; these are not available from the experiment but are important because they exert a strong influence

upon the flow. This problem was dealt with by constructing conditions representative of a transitional mixing layer and investigating their influence on the flow. Secondly, the condition at the outflow boundary is also difficult to specify. A condition that does not affect the solution upstream of the boundary was found. Thirdly and finally, a numerical method for computing the solution with these boundary conditions was constructed.

These methods will be extended to treat the axisymmetric jet. This will require the development of new numerical methods for dealing with problems in cylindrical geometry. For the mixing layer, careful experiments have shown that the two- and three-dimensional flows have different rates of mixing. This is not yet so clear for the jet, but there is reason to believe that it is true, and we shall adopt it as a working hypothesis. For this reason, we intend to do a relatively large number of two-dimensional simulations, but it is important that some three-dimensional cases be done so that comparisons of the two cases can be made.

These arguments provide the basis for the directions in which we intend to go. First, it is necessary to develop the numerical methods for dealing with axisymmetric flows. Then, simulations of completely axisymmetric jets (one with no azimuthal dependence of any of the variables) will be made. These will include flows with combustion, which will be treated by a simple model, and comparison cases without chemical reaction. All of the initial cases will be completely axisymmetric in order to reduce the computer-time requirements and turnaround time. Studies will be made of the effects of the heat-release parameter and the velocity ratio in the jet on the nature of the flame and its properties. When studies of the axisymmetric case are complete, a few carefully selected nonaxisymmetric cases will be run with a view to studying the differences between them and the completely axisymmetric cases.

We shall begin with a description of the numerical method we have developed.

B. Numerical Method for Axisymmetric Flows

The Hankel transform is ideal for numerically solving problems in axisymmetric geometry and was actively considered. The method was found useful for problems in which the solution decays rapidly with radial distance. Several numerical versions of the Hankel transform were investigated. All of these are approximations to the exact integral transform, but, unfortunately, none of them is invertible, in the sense that one cannot retrieve the original data by a second transform. Furthermore, the convergence properties of Hankel series are less than desirable.

We then decided to restrict our attention to finite geometry, in which the range of the radial variable is finite. This permits use of several families of orthogonal polynomials in the radial variable.

Some desirable properties of the polynomials are:

- Orthogonality over $(0,1)$ domain. Any domain, say, $0 \leq r \leq r_o$, can be readily transformed to this domain.
- Solutions of a Sturm-Liouville ordinary differential equation that is singular at $r = 0$ and $r = 1$. This enables application of arbitrary boundary conditions without sacrifice of spectral accuracy. For the axisymmetric problem, the radial derivative at $r = 0$ should vanish, but this is unnecessary for the nonaxisymmetric case.
- High-order members should have their zeroes clustered in regions where high resolution is desired. In our problem, this could be done at one station. However, at different downstream locations, the region requiring resolution shifts, and the polynomials may no longer be optimal.
- Polynomials should admit a fast transform, enabling easy transformation in both directions. By fast, we mean methods requiring less than $0(n^3)$ operations. At the moment, such methods are not available for our choice of polynomials.

The basis functions chosen are the normalized Jacobi polynomials. The standard Jacobi polynomials are defined for $r \in (0,1)$ and denoted by $G_n(p,q,r)$. G_n is a polynomial of degree n with weight function

$$w(r) = (1-r)^{p-q} r^{q-1} \quad ; \quad p - q > 1, \quad q > 0 \qquad (1)$$

We choose $p = q = 0.5$ so that

$$w(r) = 1/\sqrt{r} \quad . \tag{2}$$

From here on, we shall call these particular polynomials $G_n(r)$. The differential equation satisfied by them is given in [1].

$$r(1-r)\, G_n''(r) + (0.5 - 5r)\, G_n'(r) + n(n+0.5)\, G_n(r) = 0 \tag{3}$$

or, in Sturm-Liouville form,

$$[\sqrt{r}\ (1-r)\ G_n'(r)]' + n(n+0.5)\ G_n(r)/\sqrt{r} = 0 \tag{4}$$

Note that, since $P(r) \equiv \sqrt{r}\ (1-r)$ is zero at $r = 0$ and 1, the ODE (4) is singular at these points.

We chose as the basis functions:

$$H_n(r) \equiv G_n(r)/\sqrt{a_n} \tag{5}$$

so that $H_n(r)$ satisfies the orthonormality relation,

$$\int_0^1 H_n(r)\, H_m(r)\, [1/\sqrt{r}]\, dr = \delta_{nm} \tag{6}$$

The ODE (4) is also satisfied by Hn(r). The recursion relation satisfied by the H_n is:

$$rH_n(r) = H_{n+1}(r)\ \sqrt{b(n+1)} + H_n(r)\ a(n) + H_{n-1}(r)\ \sqrt{b(n)} \tag{7}$$

Using the expression for the derivative of $p_n^{(\alpha,\beta)}(r)$ [1], we can derive the following relationship satisfied by $H_n'(r)$:

$$r(1-r)H_n'(r) = H_{n+1}(r)\ d(n) + H_n(r)\ e(n) + H_{n-1}(r)\ f(n) \tag{8}$$

where

$$d(n) = -\, n\sqrt{b(n+1)}$$

$$e(n) = \frac{n^2}{(2n - 0.5)} - na(n)$$

$$f(n) = \left[\frac{2n^2\ (2n-1)\ (n-0.5)}{(4n-1)\ (4n-3)\ (2n-0.5)} - nb(n)\right]\frac{1}{\sqrt{b}(n)}$$

The zeros can be found by the method of Welsch and Golub [2].

We shall approximate a function $f(r)$ by its values at N points r_0, r_1, $\cdots$ r_{N-1}, we call the approximant $f_N(r)$ and define it by:

$$f_N(r_i) = \sum_{j=0}^{N-1} \hat{f}_j\, H_j(r_i) \quad . \tag{9}$$

Requiring that $f_N(r_i) = f(r_i)$, the exact value, leads to a system of N equations for the N unknowns $\hat{f}_o$, $\hat{f}_1$, $\cdots$ $\hat{f}_{N-1}$. This may be represented as

$$A\,\underline{\hat{f}} = \underline{f}_N \tag{1}$$

where A is a full matrix of size $N \times N$, whose elements are

$$a_{ij} = H_j(r_i) \quad , \qquad i = 0,\ 1,\ \cdots\ N-1, \quad j = 0,\ 1,\ \cdots\ ,\ (N-1)$$

The inverse of (10) is

$$\underline{\hat{f}} = A^{-1}\,\underline{f}_N \tag{11}$$

The process of finding $\underline{\hat{f}}$ from $\underline{f}_N$ is called the forward Jacobi transform; the inverse is called the (backward) Jacobi transform. In general, these transforms require operation counts of $O(N^3)$ as noted earlier.

We have not yet specified the N collocation points. If these are chosen to be the zeroes of the N^{th}-order polynomial, certain attractive properties result.

If, in Eq. (9), we remove the subscript i from r on both sides, we get a continuous function of r, an interpolant of the data provided by $\underline{f}_N(r_i)$. This interpolant is at most a polynomial of degree $(N-1)$ in r. We want to use it to estimate derivatives.

Differentiating both sides of the interpolant with respect to r and using the derivative relationship (8), we have

$$df_N/dr = \sum_{j=0}^{N-1} \hat{f}_j[d(j)H_{j+1}(r) + e(j)H_j(r) + f(j)H_{j-1}(r)]/r(1-r) \quad . \tag{12}$$

Since this is a polynomial of degree no greater than (N-2) in r, we may write

$$df_N/dr = \sum_{j=0}^{N-1} \hat{g}_j H_j(r) \tag{13}$$

Clearly, $\hat{g}_{N-1}$ must be zero. Our aim is to relate the $\hat{g}$ to the $\hat{f}$. Multiplying (13) by $r(1-r)$ and using (12),

$$\begin{aligned} r(1-r)\, df_N dr &= \sum_{j=0}^{N-1} \hat{f}_j \left[d(j)H_{j+1}(r) + e(j)H_j(r) + f(j)\, H_{j-1}(r) \right] \\ &= \sum_{j=0}^{N-1} r(1-r)\, \hat{g}_j H_j(r) \end{aligned} \tag{14}$$

By repeated use of the recurrence relation (7) followed by index shifts, we get

$$\begin{aligned} &\Sigma\, [\hat{f}_{j-1}d(j-1) + \hat{f}_j e(j) + \hat{f}_{j+1}f(j+1)]\, H_j(r) + \hat{f}_{N-1}d(N-1)H_N(r) \\ &\quad = \Sigma\, [\hat{g}_{j-2}\{-\sqrt{b(j-1)}\,\sqrt{b(j)}\} + \hat{g}_{j-1}\sqrt{b(j)}\,\{1-a(j) - a(j-1)\} + \\ &\qquad + \hat{g}_j\{a(j) - b(j+1) - a(j)^2 - b(j)\} + \hat{g}_{j+1}\sqrt{b(j+1)}\,\{1 - a(j+1) - \\ &\qquad - a(j)\} + \hat{g}_{j+2}\{-\sqrt{b(j+2)}\,\sqrt{b(j+1)}\}]\, H_j(r) + \\ &\qquad + H_N(r)\,\{\hat{g}_{N-1}\sqrt{b(N)}\,(1-a(N) - a(N-1)) - \hat{g}_{N-2}\sqrt{b(N)}\,\sqrt{b(N-1)}\} + \\ &\qquad + H_{N+1}(r)\,\{-\hat{g}_{N-1}\sqrt{b(N)}\,\sqrt{b(N+1)}\} \quad . \end{aligned} \tag{15}$$

It is assumed that, when the index on $\hat{f}$ or $\hat{g}$ falls outside the range (0,N-1), it is set to zero. Comparing coefficients of Jacobi polynomials of the same order, we get

Coefficient of $H_{N+1}(r) \rightarrow \hat{g}_{N-1} = 0$,

Coefficient of $H_N(r) \rightarrow \hat{g}_{N-2} = \hat{f}_{N-1}d(N-1)/\{-\sqrt{b(N)}\,\sqrt{b(N-1)}\}$

.

.

Coefficient of $H_2(r) \rightarrow \hat{g}_0$ can be obtained .

Thus the process of obtaining the $\hat{g}_j$, the Jacobi coefficients of df/dr is quite efficient; df/dr can then be computed by inverting $\underline{\hat{g}}$.

Using similar ideas, it is possible to obtain other derivatives of f including $d(rdf_N/dr)/dr$, which occurs in the Navier-Stokes equations.

Next, we shall consider the application of these methods to the solution of first- and second-order ODEs.

Example 2:

Consider solving a first-order ODE,

$$\frac{df(r)}{dr} = \theta(r) \tag{16a}$$

$$f(r) = f_o \tag{16b}$$

We shall use the spectral method with an (N+1) point approximation to f(r). The additional point enables us to satisfy the initial condition (16b). Thus, let us seek a solution of the form

$$f_{N+1}(r) = \sum_{j=0}^{N} \hat{f}_j H_j(r) \tag{17}$$

Let us define the inner product of two functions:

$$(f_1, f_2) \equiv \int_o^1 f_1(r)\, f_2(r) \left[1/\sqrt{r}\right] dr \tag{18}$$

(N + 1) equations for the (N + 1) unknowns $\hat{f}_o \ldots \hat{f}_N$ are needed. N equations are obtained from the N inner products,

$$\begin{gathered}(Lf_{N+1}, H_k(r)\, r(1-r)) = (\theta(r), H_k(r)\, r(1-r)) , \\ k = 0, 1, 2, \ldots, (N-1) .\end{gathered} \tag{19}$$

The last equation is derived from the initial condition:

$$f_{N+1}(0) = \sum_{j=0}^{N} \hat{f}_j H_j(0) = f_o \tag{20}$$

There are several ways of obtaining the right-hand side of (19). One could perform a quadrature for each k. We chose to sample $\theta(r)$ at N + 1

points, approximate $\theta(r)$ by an $N+1$ point approximation, and explicitly evaluate the required inner products. Equations (19) and (20) form an $N \times N$ system, which is tridiagonal plus a full last row. Special solvers may be used to solve such a system.

Example 2:

Consider Bessel's equation of order 0.

$$Lf(r) = 0 \quad , \quad L \equiv [d(rd/dr)/dr + r] \tag{21a}$$

subject to either of:

$$f(0) = J_o(0), \quad \text{or} \quad f(1) = J_o(1) \tag{21b}$$

We seek a $(N+2)$ point solution in the form,

$$f_{N+2}(r) = \sum_{j=0}^{N+1} \hat{f}_j \, H_j(r) \tag{22}$$

$(N+2)$ equations for the $(N+2)$ unknowns $\hat{f}_o \ldots \hat{f}_{N+1}$ are required. N equations are obtained from

$$\left(Lf_{N+2}, H_k(r)\, r(1-r)^2\right) = 0 \quad , \quad k = 0, \ldots, (N-) \tag{23}$$

To satisfy the boundary conditions, we set

$$f_{N+2}(0) = \sum_{j=0}^{N+1} f_j \, H_j(0) = J_o(0) \tag{24a}$$

$$f_{N+2}(1) = \sum_{j=0}^{N+1} \hat{f}_j \, H_j(1) = J_o(1) \tag{24b}$$

Thus, we obtain a matrix system for $\underline{\hat{f}}$. This matrix is sparse, having entries along nine of its diagonals, as well as its last two rows. Again, we can utilize special matrix solvers.

III. Turbulent Flame Propagation

A. Physics of Turbulent Flames

The propagation of a flame front into a premixed fuel-oxidant mixture is important in a number of situations, including some types of gas turbine and internal combustion engines. The stability of such flames and the issues of ignition and extinction are other important issues in turbulent flame propagation. The importance of turbulent flame propagation and its difference from the axisymmetric jet problem described above made this problem our choice as the second case to be simulated.

In all cases of interest in applications, the flame front is thin with respect to most of the other length scales of importance in the problem. In particular, actual flames are always thin with respect to the largest length scales of the turbulence. Whether they are smaller than the finest scales of the turbulence or not depends on such parameters as the Damkohler and Reynolds numbers. Both cases are of interest and importance and have been considered. The approaches to simulating the two cases differ somewhat.

If the flame is thick with respect to the smallest scale of the turbulence (the Kolmogoroff scale), the appropriate approach is full simulation in which the chemical equations are solved together with the Navier-Stokes equations; all of the details are then resolved on a single grid. This is very similar to the approach that has been used in nonreacting flows. However, with the computer resources available today, the parameter range accessible to this method is rather limited.

On the other hand, if the flame is thin with respect to the Kolmogoroff scale, it is more efficient to use an approach in which the outer flow and the flame are computed on different scales and the solutions are matched. In this approach, the flame appears to be a thin discontinuity to the outer flow. The flame is computed on a smaller scale in which the flow appears laminar but may be unsteady, stretched, and/or curved. In this method, effort can be saved by precomputing the properties of the flame. This approach requires development of a method of dealing with discontinuities, as previous simulations of nonreacting turbulent flows have not required this feature.

Because it offers the possibility of handling high Damkohler numbers, we expect to use the second approach but are reserving the possibility that the

first approach will be needed in the future. The method will be used to study the geometry of the flame front and its average speed of propagation as a function of various parameters (including the laminar flame speed and the length scales and intensity of the turbulence).

B. Laminar Flame Calculations

We have investigated several algorithms for solving the laminar flame problem in order to gain experience solving the equations, including solving both the unsteady and steady problems. We used a global, single-step kinetics model and assumed Lewis number unity. A test problem from Peters and Warnatz [3] served as the test. The nondimensional equations listed below were used to describe the laminar flame.

$$\frac{\partial \rho}{\partial t} + \frac{\partial \rho u}{\partial x} = 0$$

$$\frac{\partial \rho u}{\partial t} + \frac{\partial \rho u^2}{\partial x} = - \frac{\partial P^{(1)}}{\partial x}$$

$$\frac{\partial \rho T}{\partial t} + \frac{\partial \rho u T}{\partial x} = D \frac{\partial^2 T}{\partial x^2} + \dot{W}$$

$$\frac{\partial \rho Y}{\partial t} + \frac{\partial \rho u Y}{\partial x} = D \frac{\partial^2 Y}{\partial x^2} - \dot{W}$$

$$p^{(0)} = \rho T = \text{constant}$$

where $\dot{W} = B\, Y \exp(-\beta(1-T)/(1-\alpha(1-T)))$ is the reaction rate,

β is the nondimensional activation energy,

B is the Damkohler number, and

α is the nondimensional heat release.

For the unsteady problem, we used numerical techniques which could be extended to the multidimensional turbulent problem. Specifically, we used second-order central finite differences for the spatial derivatives and second-order Adams-Bashforth for the time integration. The unsteady problem

was solved with and without the convection terms in the energy equation. With the convection terms included, the problem is fairly difficult. This is discussed below.

Solving the equations without the convection terms was fairly easy. In the standard method, the troublesome terms are removed by an appropriate coordinate transformation:

$$\bar{t} = t \ , \quad \bar{x} = \int_0^x \rho \, dx$$

where the overbar signifies the transformed coordinates. Unfortunately, this transformation cannot be used in higher dimensions. For the constant pressure case, the resulting equations are greatly simplified:

$$\frac{\partial \rho T}{\partial \bar{t}} = D_{th} \frac{\partial^2 T}{\partial \bar{x}^2} + \dot{W}$$

$$\frac{\partial \rho Y}{\partial \bar{t}} = D_M \frac{\partial^2 Y}{\partial \bar{x}^2} - \dot{W}$$

Using these equations, the internal structure of the flame is fairly easy to calculate, but the flame speed is extremely sensitive to the acccuracy of the calculation. The flame structure and speed from sample calculations are shown in Figs. 1-4. The structure appears well resolved with either 200 or 400 points. However, the flame speed oscillates and the amplitude of oscillation depends on the number of points. The oscillations are due to small changes in the chemical source term as it propagates over the grid. Since the flame speed is dependent on the total heat release in the flame, these small changes are significant enough to cause the oscillations. The sensitivity of the laminar flame calculation to the source term indicates that special techniques such as grid refinement or grid adaptation will be very helpful.

We also worked on solution techniques for the steady equations. The approach was to recast the constant-pressure problem as a system of ODEs and use standard subroutines to solve the system. The classical cold boundary problem now appears because the steady problem is actually ill-posed.

First, we used a shooting technique. This involved guessing the initial temperature gradient and the flame speed, and integrating the equations through the flame. Correct initial guesses result in zero temperature gra-

dient at the end of the flame. As is usual for stiff problems, shooting did not work very well. The problem could be written:

Solve:	Initial Conditions:
$g_1' = g_2$	$g_1(0) = 0$
$g_2' = \rho u g_1 - \dot{W}$	$g_2(0) =$ small initial guess

where $g_1 \equiv T$

$g_2 \equiv dT/dx$

$\dot{W} \equiv B(1-T)\exp(-\beta(1-T)/(1-\alpha(1-T)))$

We had more success by posing the problem as a boundary-value problem and using a subroutine written by V. Pereyra called DVCPR. In this case, the flame-speed eigenvalue was treated as an unknown and another equation was added to the system.

Define:	Solve:	Boundary Conditions:
$g_1 \equiv T$	$g_1' = g_2$	$g_1(0) = 0$
$g_2 \equiv \frac{dT}{dx}$	$g_2' = g_3 g_2 - \dot{W}$	$g_1(L) = 1$
$g_3 \equiv \rho u$	$g_3' = 0$	$g_2(L) = 0$

Adding the extra equation not only gives the desired solution without iteration, but it also allows an extra boundary condition to be enforced. This is highly desirable. This method worked very well, and the results were consistent with the Peters test problem results. For example, with a Damkohler number of 50 and a nondimensional activation energy of 10, the flame velocity was 0.917, while the values reported by others ranged from 0.894 to 0.918.

C. Evaluation of Numerical Methods

We are restricting attention to low-speed flows to allow computations to be made without modeling. This is a common approach (Merkle and Choi [5]), so we shall list the nondimensionalized equations without development:

$$\frac{\partial \rho}{\partial t} + \frac{\partial \rho u_i}{\partial x_i} = 0$$

$$\frac{\partial \rho u_i}{\partial t} + \frac{\partial \rho u_j u_i}{\partial x_j} = -\frac{\partial P^{(1)}}{\partial x_i} + \frac{\partial \tau_{ji}}{\partial x_j}$$

$$\frac{\partial \rho T}{\partial t} + \frac{\partial \rho u_j T}{\partial x_j} = D_{th} \frac{\partial^2 T}{\partial x_j \partial x_j} + \dot{W} \qquad (25)$$

$$\frac{\partial \rho Y}{\partial t} + \frac{\partial \rho u_j Y}{\partial x_j} = D_M \frac{\partial^2 Y}{\partial x_j \partial x_j} - \dot{W}$$

$$P^{(0)} = \rho T = \text{constant}$$

where: τ_{ji} = shear stress,

D_{th} = thermal diffusivity,

D_M = mass diffusivity, and

$\dot{W}$ = chemical source term, $f(Y,T)$.

To find an effective numerical solution technique for these equations, we face two problems. Both arise from the decoupling of the thermodynamic pressure, $P^{(0)}$, from the kinematic pressure, $P^{(1)}$, in the low Mach number approximation and the density variation.

One problem is best examined by combining the energy and the state equations. The result is

$$\frac{\partial u_j}{\partial x_j} = \frac{1}{P^{(0)}} D_{th} \frac{\partial^2 T}{\partial x_j \partial x_j} + \dot{W} \qquad (26)$$

which clearly shows the main effect of the combustion on the velocity field. The problem arises from the lack of a time derivative in this equation. We have approached this problem in two ways.

In the first approach, we use the idea from incompressible flow that this equation is enforced via a Poisson equation for the pressure. Thus we take the divergence of the momentum equation and attempt to enforce Eq. (26) in the resulting equation. This approach could take several forms. We are examining the idea of decomposing the velocity field into two parts: one from the energy equation and one that is divergence-free. We are also looking at using a global projection operation similar to a "weak" formulation of the momentum equation [7]. Work is just beginning on this approach, and we have not yet found a suitable method.

In the second approach, we solve one equation in nonconservative form; either the energy equation or the continuity equation could be treated this way. McMurtry et al. [4] solve the continuity equation in nonconservative form and use the energy equation to replace the velocity divergence. Numerically solving an equation in nonconservative form requires extra care to assure the global conservation of certain quantities such as energy. In the low Mach number equations, we have the added difficulty that kinetic and thermal/chemical energy must be independently conserved. We would prefer to avoid nonconservative schemes if a suitable scheme can be found.

The second problem which arises in solving the low Mach number equations concerns the Poisson equation for the pressure. When we take the divergence of the numerical momentum equation, the following term appears:

$$\frac{\delta \rho u_i}{\delta x_i}^{n+1} \qquad \text{(where } \delta \text{ is a numerical operator)}$$

For incompressible flows, this term is zero by continuity. If we use continuity for this term in the low Mach number equations, we have to approximate the term:

$$-\frac{\delta \rho}{\delta t}^{n+1}$$

McMurtry uses this approach and approximates this term by backward differencing. While this approach works, it would be better to avoid a numerical approximation of a time derivative in the Poisson equation.

Finally, we note that these problems can be avoided completely by not using the low Mach number approximation. This would result in a new set of

problems. For example, in low-speed flows the time-step limitation can be severe. One approach used in low-speed compressible flows is to use acoustic subcycling and filtering. This approach is used by O'Rourke [6] and involves resolving the sound waves by integrating a subset of the equations over many small time steps during one regular time step. While this may work, it is too inefficient for our requirements.

D. Two-Dimensional Code Development

We are now developing a code for 2-D turbulent reacting flows. It is based on McMurtry's method, but this will be changed when we develop something better. The code is for premixed flames and uses single-step global kinetics. It is a full simulation code and thus has no modeling. In the streamwise direction we are using finite differences, because there are inflow and outflow boundary conditions. In the spanwise direction, the boundaries are periodic, so a Fourier spectral method is used. The variable density Navier-Stokes solver and Poisson pressure solver are completed and in the testing phase. Solvers for the energy and species equations remain to be written but should be straightforward.

References

1. Abramowitz, M., and I. A. Stegun, Handbook of Mathematical Functions with Formulas, Graphs, and Mathematical Tables, National Bureau of Standards Applied Mathematics Series 55, 1972.

2. Golub, G. H., and J. H. Welsch, "Calculation of Gauss Quadrature Rules," Math. of Comp., **29**: 221-230, 1969.

3. Numerical Methods in Laminar Flame Propagation (N. Peters and J. Warnatz, eds.), Friedr. Vieweg & Sohn, 1982.

4. McMurtry, P. A., W. H. Jou, J. J. Riley, and R. W. Metcalfe, "Direct Numerical Simulations of a Reacting Mixing Layer with Chemical Heat Release," AIAA-85-0143, 1985.

5. Merkle, C. L., and Y-H. Choi, "Computation of Compressible Flows at Very Low Mach Numbers," AIAA-86-0351, 1985.

6. O'Rourke, P. J., "The KIVA Computer Program for Multidimensional Chemically Reactive Fluid Flows with Fuel Sprays," Numerical Simulation of Combustion Phenomena (R. Glowinski, B. Larrouturou, and R. Teman, eds.), Springer-Verlag, 1985, pp. 74-89.

7. Moser, R. D., and P. Moin, "Direct Numerical Simulation of Curved Turbulent Channel Flow," Rept. No. TF-20, Thermosciences Division, Department of Mechanical Engineering, Stanford University, 1984.

Figure 1

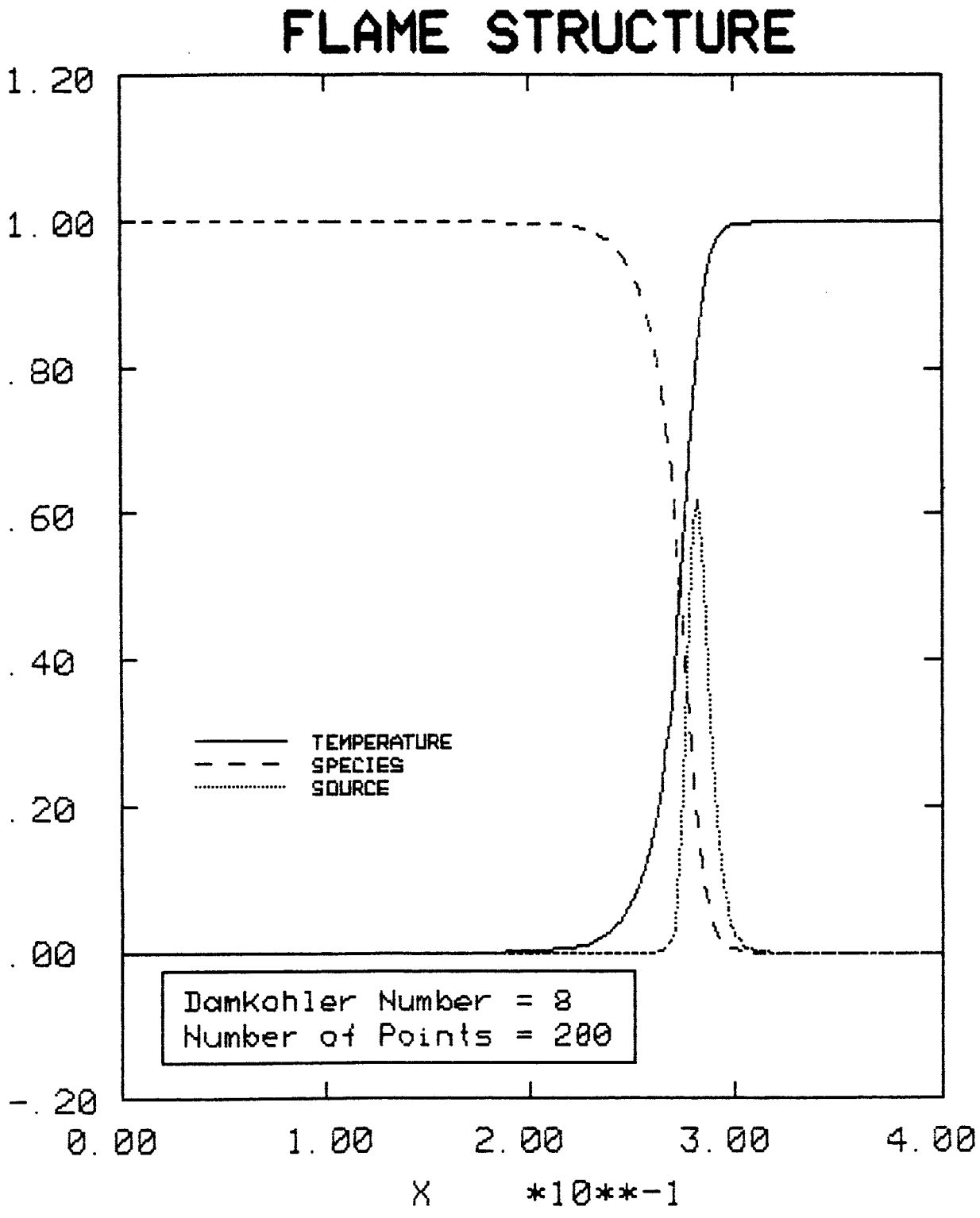

11.46.15
11-JUL-86

Figure 2

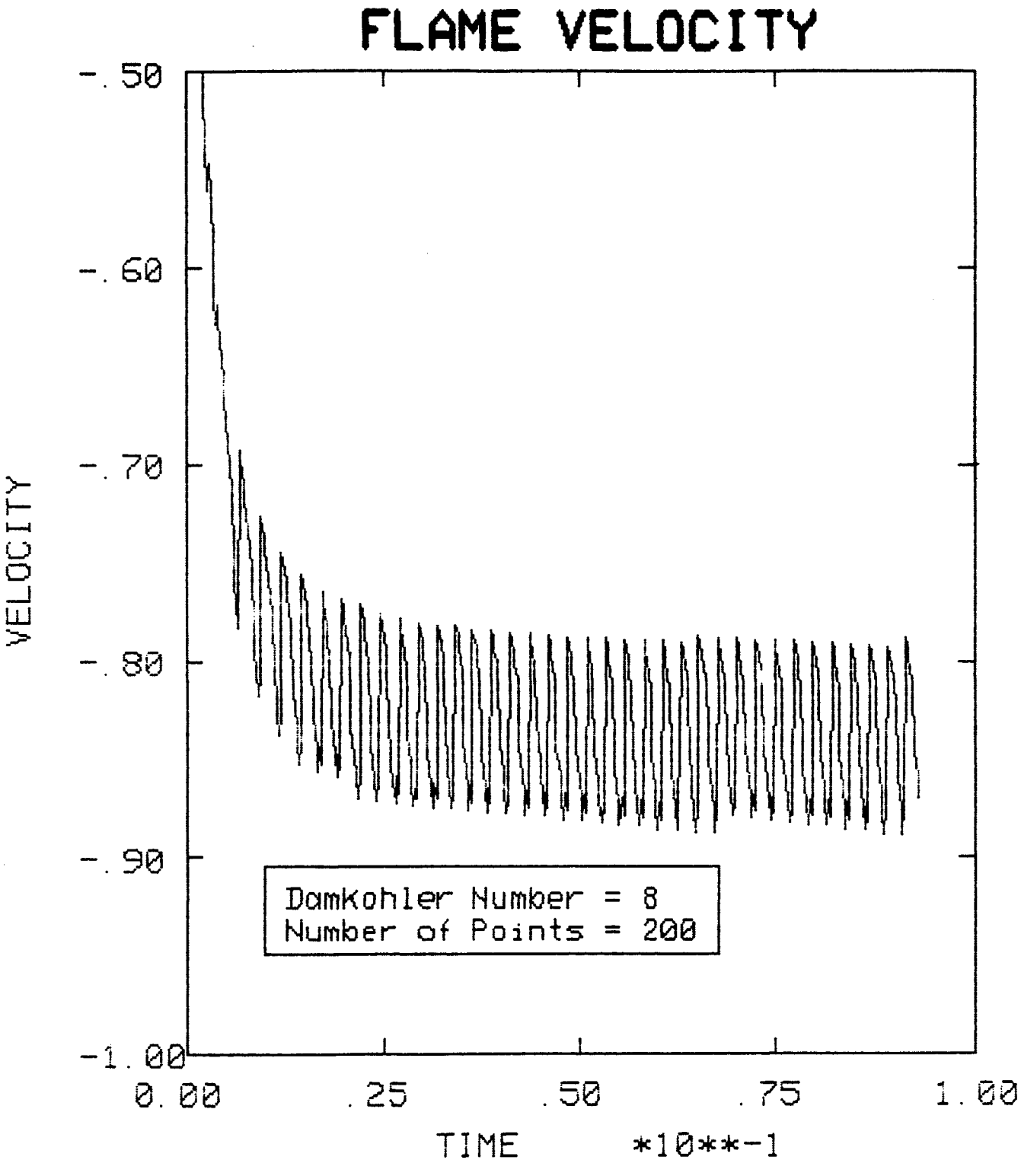

11.29.54
11-JUL-86

Figure 3

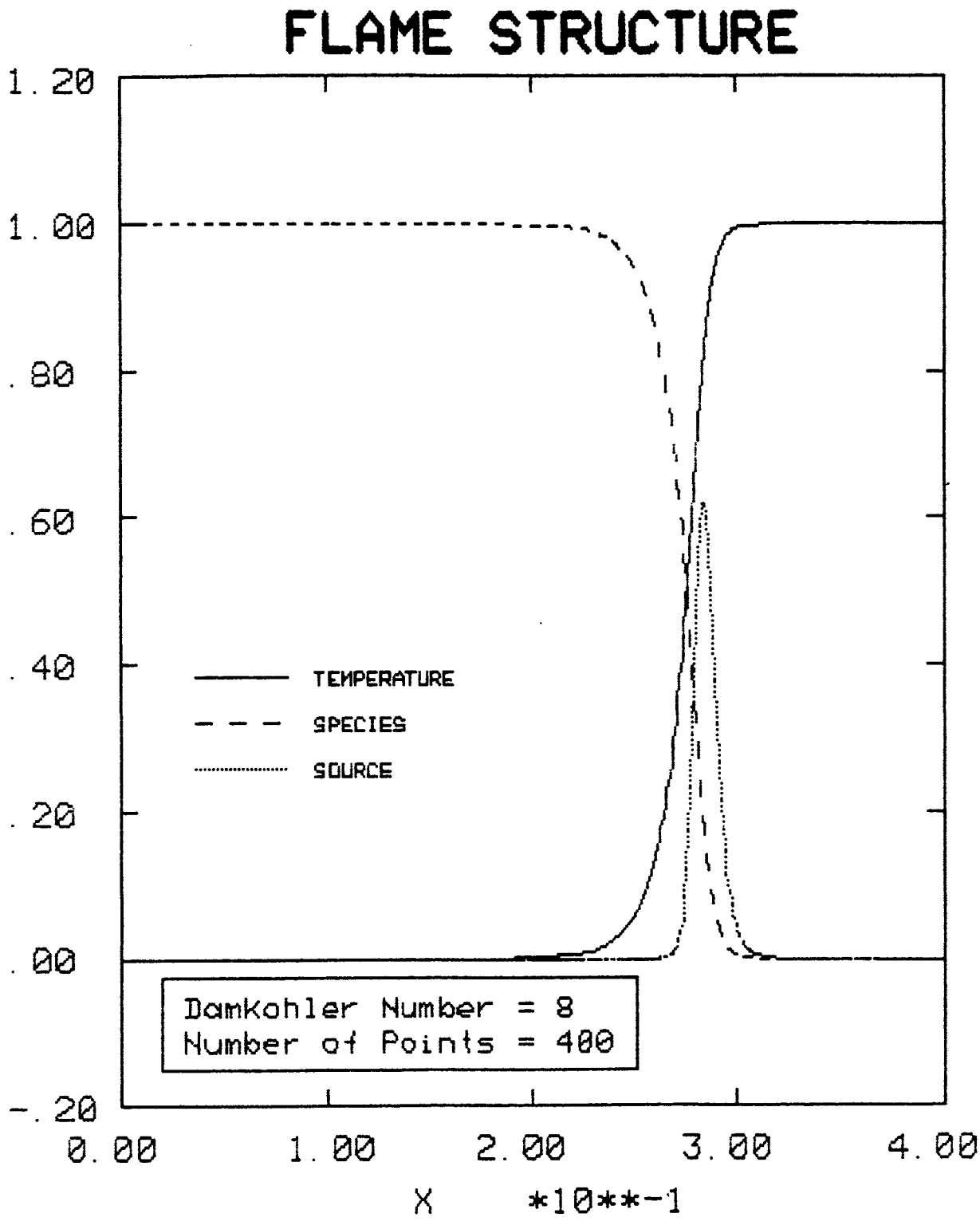

11.01.08
11-JUL-86

Figure 4

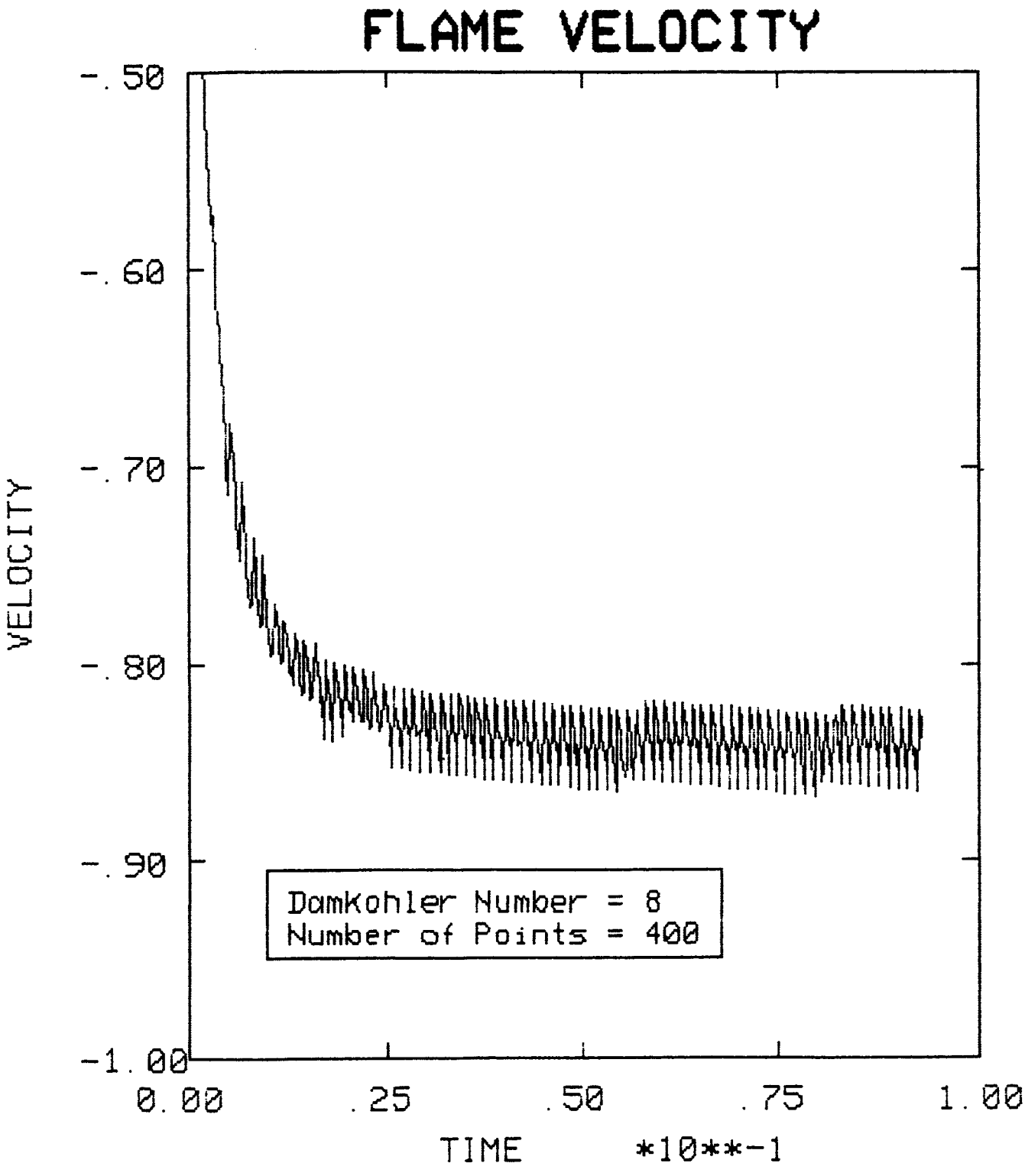

10.38.46
11-JUL-86